NUCLEAR INSTRUMENTS AND METHODS 152 (1978) 23-29 , © NORTH-HOLLAND PUBLISHING CO

A PROPOSAL TO INSTALL A SUPERCONDUCTING WIGGLER MAGNET ON THE STORAGE RING VEPP-3 FOR GENERATION OF THE SYNCHROTRON RADIATION

L M BARKOV, V B BARYSHEV, G N KULIPANOV, N A MEZENTSEV
V F PINDYURIN, A N SKRINSKY and V M KHOREV

Institute of Nuclear Physics, Novosibirsk 90, 63090, U S S R

A proposal is discussed to install a superconducting wiggler magnet on the storage ring VEPP-3 in order to shift the spectrum of the synchrotron radiation generated to a shorter wavelength range and to enhance the SR intensity The basic considerations are presented for optioned wiggler parameters aimed at the maximum brightness of the source in the range of $\lambda \approx 1$ Å The characteristics of the SR beam generated by the wiggler have been calculated (i e total power radiated, spectral and angular distribution)

A 20-pole wiggler design is presented with the length of 1 m, maximum magnetic field strength of 40 kGs, poles spaced by 16 mm and vertical aperture accessible for the electron beam of about 8 mm The intended wiggler installation scheme in a storage ring straight section envisages the storage of electrons apart from the wiggler aperture using the complete admittance of the storage ring with the subsequent shift of the stored beam into the wiggler by means of the localized closed orbit distortion

The influence of the wiggler field on particles motion in the storage ring has been considered (e g closed orbit distortion, betatron oscillations frequency shift, contribution to the cubic nonlinearity etc)

1. Introduction

Practically all the storage rings used up-to-date for the synchrotron radiation research were primarily designed as colliding beams facilities In spite of being good short-wave radiation sources these machines undoubtedly are not optimal generators to produce the synchrotron radiation (SR)

One of the very effective means to improve the SR parameters on the existing storage rings is to install a wiggler magnet[1-7]) which produces an alternating magnetic field on a part of an orbit therefore providing the concentration in the SR beam of the radiation from a long path of the orbit The application of the wiggler (in Russian called "snake") may be profitable in various problems concerning the SR generation

- creation of superhigh power short-wave SR beams,
- high efficiency RF power conversion into SR,
- enhancement in brightness of SR beams (generation of the intense SR beams with small emittance),
- transformation of the SR spectral characteristics (enhancement of the spectral density in a given spectral range, reduction of the short-wave band etc),
- generation of SR beams with needed polarization

Especially interesting is the proposal to install a wiggler in a storage ring to create a free electron laser[8]).

The wiggler parameters (i e the strength of the magnetic field, period length $2b$, total length L_w) depend on the problem in question Two extreme cases are easily seen in wiggler applications

1) with ultimately high field (up to 60–100 kG) to achieve a maximum SR quantum energy in an existing storage ring,
2) with extremely short period of field variation and low field (0 1–1 kG) to generate so-called "ondulatory" radiation[4,5])

In the present paper a variant of the wiggler installation on the VEPP-3 storage ring is considered which occupied ≈ 1 m along the orbit, with relatively high field of ≈ 35 kG, small spatial periodicity length ($2b = 9$ cm) and small vertical aperture of 16 mm The optioned wiggler parameters are aimed at the SR brightness enhancement in the range of $\lambda \approx 1$ Å

2. The principal characteristics of the SR generated in a wiggler

For wigglers with high fields the radiation formation length is much less than that of the field variation periodicity Thus the SR generated in the given point of the orbit is characterized by the local path curvature For description of the radiation generated in the wiggler the conventional SR the-

ory (assuming electrons to move circularly) formulae are valid if properly integrated over the electron path To simplify the situation we assume that an observation point lies at a distance much greater than the wiggler length

The vertical component of the magnetic field in the vicinity of the wiggler axis may be written as follows.

$$H_z(s) = H_0 \sin\frac{\pi s}{b}, \tag{1}$$

where s is the longitudinal coordinate,
$2b$ is the field variation period length;
H_0 stands for the maximum field

The electron trajectory in the wiggler may be described by the deviation $x(s)$ of the electron path from the axis and by the angle $x'(s)$ between the electron velocity and the axis (see fig 1).

$$x(s) = x_0 \sin\frac{\pi s}{b}, \qquad x'(s) = \alpha_0 \cos\frac{\pi s}{b}, \tag{2}$$

where

$$\alpha_0 = \frac{eH_0 b}{\pi E}, \quad \alpha_0[\text{mrad}] = 9.5\times10^{-2}\,\frac{H_0[kG]\,b[\text{cm}]}{E[\text{GeV}]}, \tag{3}$$

$$x_0 = \frac{\alpha_0 b}{\pi} = \frac{eH_0 b^2}{\pi^2 E},$$

$$x_0[\text{mm}] = 3\times10^{-4}\,\frac{H_0[\text{kG}]\,b^2[\text{cm}]}{E[\text{GeV}]} \tag{4}$$

Making use of the relation for the total SR power in case of an ultrarelativistic electron[9]) and accounting for eq. (1) we find out the electron energy lost on synchrotron radiation.

$$\dot{W}[\text{W}] = 1.3\times10^{-4}E^2[\text{GeV}]\,H_0^2[\text{kG}]\,I[\text{mA}]\,b[\text{cm}]\,n; \tag{5}$$

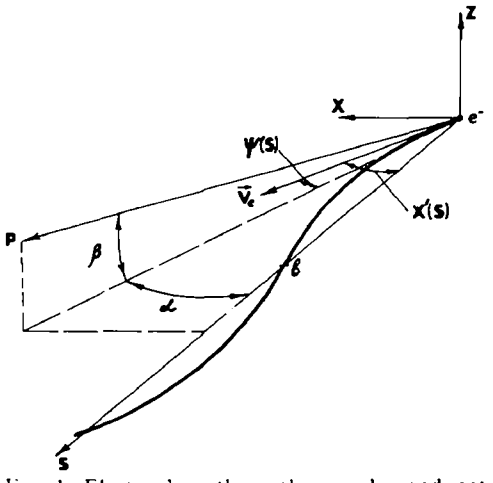

Fig 1 Electron's path in the wiggler and notations

here E stands for the electron energy in a storage ring, I is the electron current, $n = L_w/2b$ – total number of the wiggler periods

An essential characteristic of radiation is the spectral photon flux $N(\lambda)$ or the spectral power $W(\lambda)$[7]) – taken at a given wavelength λ in $\Delta\lambda/\lambda$ range By integration of the formula for power spectrum of the synchrotron radiation[9]) over the electron path in the wiggler we obtain, with the account of eq (1)

$$\dot{N}(\lambda)\left[\frac{\text{photons}}{\text{sec}}\right] = 1.5\times10^{13}H_0[\text{kG}]\,nb[\text{cm}]\times$$

$$\times\, I[\text{mA}]\,\eta_w(y_0)\,\frac{\Delta\lambda}{\lambda}, \tag{6}$$

$$\dot{W}(\lambda)\,[\text{W}] = 1.46\times10^{-2}\,H_0[\text{kG}]\,\frac{2nb[\text{cm}]}{\lambda[\text{Å}]}\times$$

$$\times\, I[\text{mA}]\,\eta_w(y_0)\,\frac{\Delta\lambda}{\lambda}, \tag{7}$$

where $y = \lambda_c/\lambda$, $\lambda_c = 4\pi mc^2/3eH_0\gamma^2$ is the critical SR wavelength[7]) at maximum magnetic field H_0, $\eta_w(y_0)$ is a universal spectral function of the wiggler radiation[7]) plotted in fig. 2.

The spectral and angular distribution of radiated power in the wiggler center plane integrated over the vertical angle β is of interest. It results from the integration of the instantaneous spectral and angular distribution of the SR power[9]) over β and electron's path in the wiggler with the account of $\psi = \mathrm{d} - x'(s)$. In the case of $\alpha_0 \gg 1/\gamma$ that is of particular interest (i e the bend angle in one wiggler sector is much greater than the radiation formation angle) the angular distribution of power is determined uniquely by the electron's path in the wiggler and the radiated power at angles $\alpha > \alpha_0$

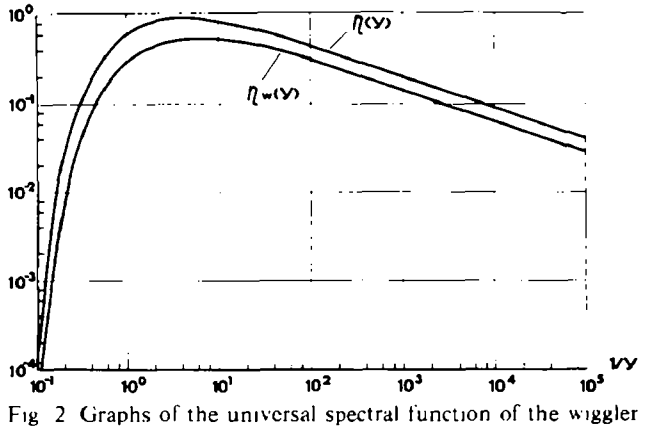

Fig 2 Graphs of the universal spectral function of the wiggler radiation and its analogue in circular motion

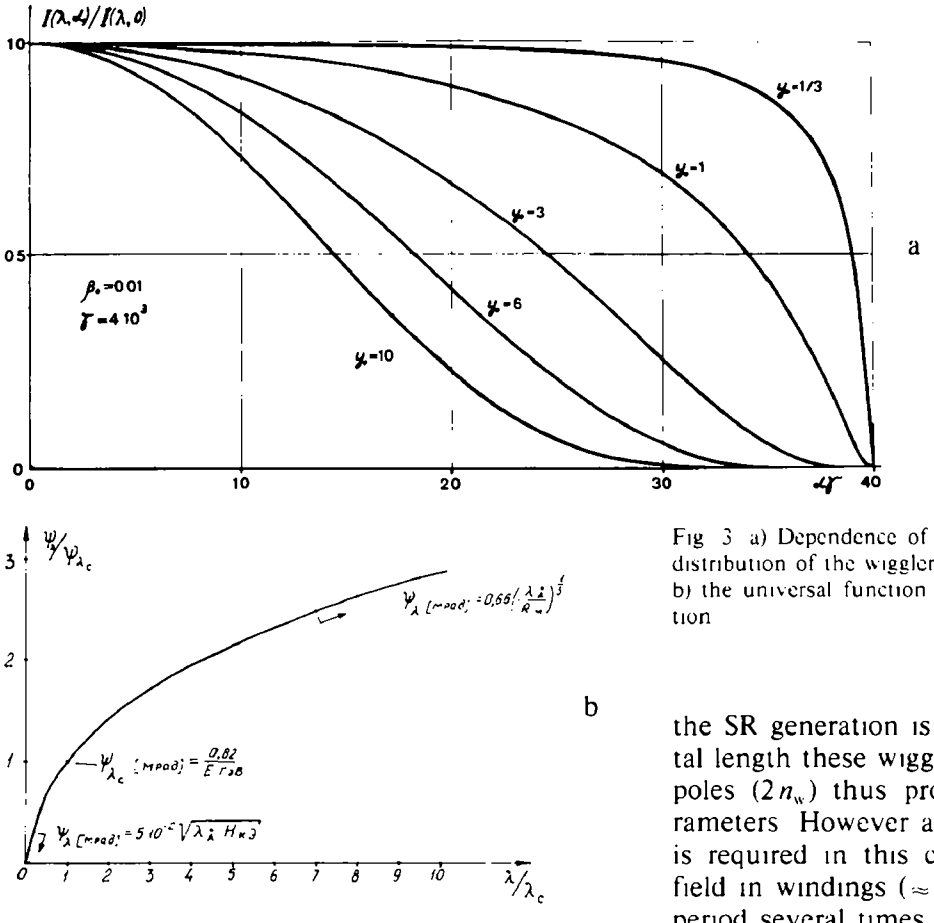

Fig 3 a) Dependence of the normalized spectral and angular distribution of the wiggler radiation on the horizontal angle α, b) the universal function for SR beam vertical angle distribution

vanishes The dependence of radiation power normalized by that radiated at zero angle $I(\alpha, \lambda)/I(0, \lambda)$ on the horizontal angle α expressed in terms of I/γ at $\alpha_0 = 0.01$ and $\gamma = 4 \times 10^3$ is shown in fig 3a at various values of y_0

The spectral and angular distribution of radiation power in the vertical plane is similar to the case of circular motion Therefore the angular divergence of radiation in the vertical plane may be determined as usual[7]).

$$2\beta_0\,[\text{mrad}] = \frac{0.82}{E[\text{GeV}]}\,\xi\left(\frac{1}{y_0}\right), \qquad (8)$$

where $\xi(1/y_0)$ is a universal function plotted in fig 3b

The main parameters of the SR beam from the superconductive wiggler ($H_0 = 35$ kG, $2b = 9$ cm, $n = 10$) to be installed in VEPP-3 ($E = 2$ Gev, $I = 100$ mA) are presented in table 1

3. The influence of the wiggler on particle motion in a storage ring

In consideration of various wiggler versions the advantage of small field variation period ones in the SR generation is obvious because at given total length these wigglers have a greater number of poles ($2n_w$) thus providing higher SR beam parameters However a smaller vertical aperture size is required in this case as at a given maximum field in windings (≈ 80 kG) one has to design the period several times longer than the vertical aperture size to generate the field of 30–50 kG on the electron's path

The minimization of the gap makes good because the helium-cooled volume and the installation overall dimensions get less, reducing the stored energy and facilitating the wiggler operation On the other hand a small size of the vacuum chamber in the wiggler makes it difficult to stack electrons

For efficient electrons stack the proposed scheme of wiggler installation in a VEPP-3

TABLE 1

Characteristics of the SR beam from the VEPP-3 superconducting wiggler

Total SR power radiated in wiggler (kW)	2.8
SR beam horizontal divergence (mrad)	17
SR beam vertical divergence (mrad)	0.4
Beam size at the SR beam line exit (mm²)	70×1.6
Critical wavelength of the synchrotron radiation (Å)	1.33
Illumination at the SR beam line exit in the λ range 0.3–3 Å (photons/sec mm²)	(1–4) 10^{16}

straight section envisages to store electrons apart from the wiggler aperture using the complete admittance of the storage ring After storage of the needed current the energy is brought up and the electron beam of small size due to damping is shifted into the wiggler by several orbit corrections (see fig 4)

Correctors are steered so as to avoid orbit distortions in the rest of the orbit. Two additional magnets at either wiggler end bend the orbit through the angle of $\alpha_0/2$ thus providing a beam position independent of the wiggler field strength. After the correction the wiggler field is gradually brought up in accordance with the additional magnets.

The wiggler magnetic field in the vicinity of the beam path can be approximately described by

$$H_X = -H_0 \sin\frac{\pi X}{a} \sin\frac{\pi S}{b}\left(\frac{\pi}{a} Z + K_X Z^3 + \ldots\right),$$

$$H_Z = H_0 \cos\frac{\pi X}{a} \sin\frac{\pi S}{b} \times$$

$$\times\left[1 + \frac{\pi^2(a^2+b^2)}{2a^2b^2} Z^2 + \ldots\right], \qquad (9)$$

$$H_S = H_0 \cos\frac{\pi X}{a} \cos\frac{\pi S}{b}\left(\frac{\pi}{b} Z + K_S Z^3 + \ldots\right),$$

where X, Z, S are radial, vertical and longitudinal coordinates, respectively, a is the effective radial dimension of the wiggler, K_x and K_s are the multipole expansion coefficients of H_x and H_s.

Analyzing the wiggler field influence on particle dynamics one comes to the evident conclusions

1) The equilibrium particle travelling in the wiggler with $Z = 0$ sees only $H_{Z_0} = H_0 \cos(\pi X/a) \sin(\pi S/b)$, its path in the wiggler is determined by H_{Z_0} (deviations in angle and coordinate $X'(S)$ and $X(S)$ given by refs 3 and 4)
2) The wiggler causes an additional focussing, the inverse of the effective focussing length (vertical plane) is

$$1/F_Z = \frac{H_0^2 b}{(HR)^2}\left(1 + \frac{b^2}{a^2}\right) n. \qquad (10)$$

The first term in brackets is due to the fringe field focussing, the second one results from non-zero horizontal position of the equilibrium particle path (i.e. at $X \neq 0$ the sextupole term in the H_Z expansion produces a quadrupole field which results in the vertical focussing and horizontal defocussing)

In the horizontal plane

$$1/F_X = -\frac{H_0^2 b^3}{(HR)^2 a^2} n \qquad (11)$$

In horizontal betatron oscillations weak focussing due to bending of the particle path cancels the fringe field effect

Eqs (10) and (11) are valid if $F_{X,Z} \gg L_w$ The higher-order multipoles effect is negligible cut by high powers of the small parameter $H_0 b/(HR) \approx 10^{-2}$

The betatron time shifts can be essessed from the wellknown relation

$$\Delta\nu_{X,Z} = \frac{1}{4\pi}\frac{\beta_{X,Z}}{F_{X,Z}},$$

where $\Delta\nu_{X,Z}$ is time-shift of either horizontal or vertical oscillation, $\beta_{X,Z}$ stands for β-function in the unperturbed storage ring lattice in the place of the wiggler location

The time-shifts are determined by

$$\Delta\nu_X = -\frac{\beta_X H_0^2 b^3}{4\pi (HR)^2 a^2} n, \qquad (13)$$

$$\Delta\nu_Z = \frac{\beta_Z H_0^2 b}{4\pi (HR)^2}\left(1 + \frac{b^2}{a^2}\right) n \qquad (14)$$

stands for the number of periods of the wiggler

The tune-shifts are to be compensated by a variation of the quadrupole lenses excitation in accordance with the wiggler field turning-on This will be made in the straight section where the wiggler is to be located and where the quadrupoles are supplied and steered individually

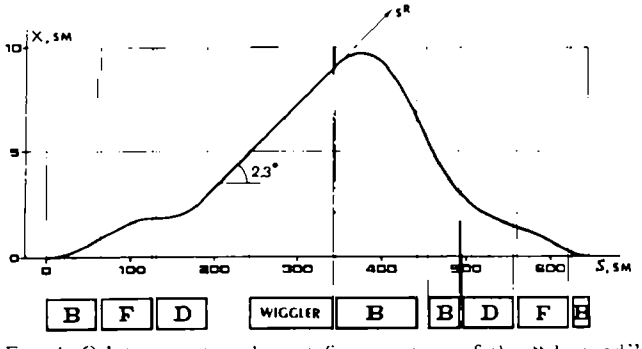

Fig 4 Orbit correction layout for insertion of the "damped" electron beam into the wiggler field area

3) The second-order term in respect of Z in H_Z expansion and the third-order term in H_X, H_S expansions cause the dependence of the wiggler focussing strength on the vertical betatron oscillations amplitude thus yielding $\partial \nu_Z / \partial a^2 \neq 0$

Terms $\sim X^4$ in H_Z expansion and account of the horizontal excursions of the equilibrium particle path in the wiggler give rise to the dependence of the wiggler focussing strength on the amplitude of the horizontal betatron oscillations therefore $\partial \nu_X / \partial a^2_X$ and $\partial \nu_Z / \partial a^2_Z$ arise The cubic nonlinearities resulting from the wiggler field can be estimated readily

$$\frac{\partial \nu_X}{\partial a_X^2} = \frac{3\pi}{32} \frac{\beta_X H_0^2 b^3}{(HR)^2 a^4}, \tag{15}$$

$$\frac{\partial \nu_Z}{\partial a_Z^2} = \frac{3\pi}{32} \frac{\beta_Z H_0^2 (a^2+b^2)^2}{(HR)^2 a^4 b}. \tag{16}$$

One can reason from eqs (15) and (16) that increase in a always reduces the tune-shifts and the cubic-nonlinearities Requirements of fairly good beam lifetime put on the cubic nonlinearities result in setting a low limit on a

For the VEPP-3 storage ring with β-functions in the wiggler location of $\beta_X = \beta_Z = 200$ cm and wiggler parameters $H_0 = 35$ kG, $b = 4.5$ cm, $a = 6$ cm and $n = 10$ estimates of the tune shifts and cubic nonlinearities give

$$\frac{\partial \nu_X}{\partial a_X^2} \approx 1.5 \times 10^{-3}\ \text{cm}^{-2}, \qquad \Delta \nu_X \approx 2 \times 10^{-2},$$

$$\frac{\partial \nu_Z}{\partial a_Z^2} \approx 1 \times 10^{-2}\ \text{cm}^{-2}, \qquad \Delta \nu_Z \approx -0.1$$

4. Design of the wiggler proposed for VEPP-3

At present the VEPP-3 wiggler is under designing and model testing.

Its magnetic structure is composed of 20 pairs of superconducting magnets which generate alternating 35 kG field 4.5 cm half-period In the magnet design the special care is taken of the minimizing the superconducting magnets dimensions and of options to mount and to remove the wiggler without disturbance of the storage ring vacuum chamber

The wiggler design schematic view is presented in fig 5 According to stacking technique described above the vacuum chamber sector (6) inside the wiggler consists of two adjacent parts different in vertical aperture size The smaller one (5) inserted in the superconducting magnets field The provisions are made to cool the vacuum

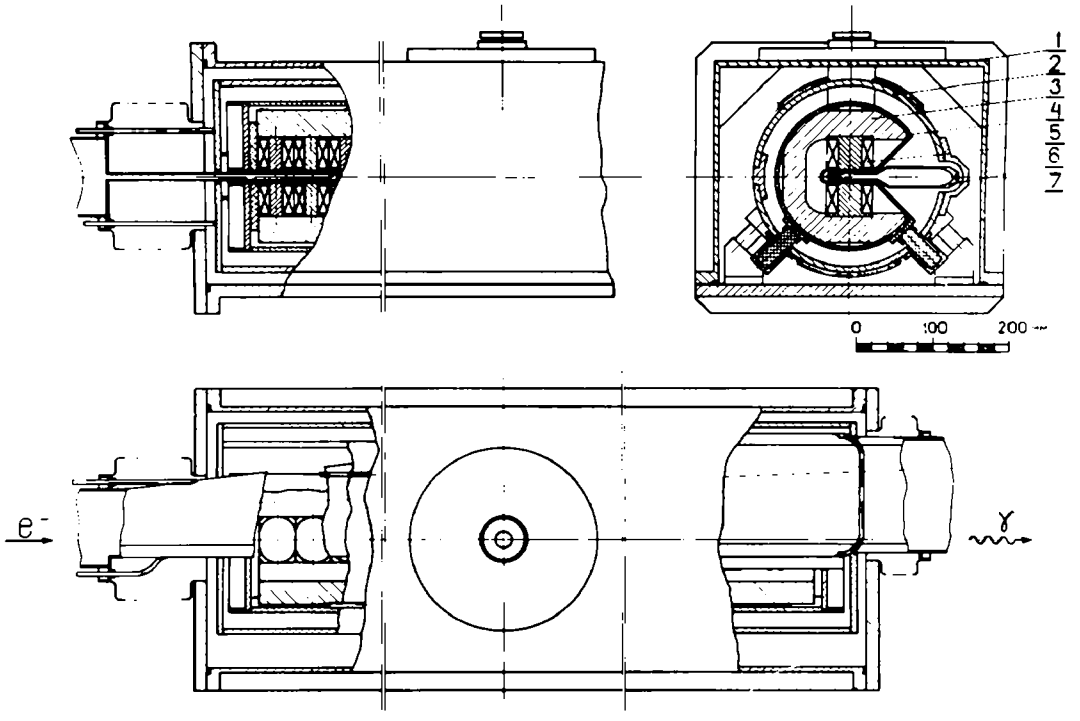

Fig 5 Schematic view of the wiggler design

TABLE 2
Parameters of the superconducting magnets

Magnetic field amplitude on beam axis (kG)	35
Number of the superconducting magnets	40
Number of the field variation periods	10
Field half-period length (cm)	4 5
The superconducting winding overall dimensions (cm)	
along beam line	4 5
across beam line	6 0
height	3 7
Designed current density (kA/cm^2)	3 2
Total energy stored (kJ)	20
Cable diameter (mm)	0 7
Operational current (A)	220
Magnet pole gap (cm)	1 5
Vacuum chamber vertical aperture size in wiggler (cm)	0 76
Total length occupied by field (m)	0 9

chamber walls with liquid nitrogene so as to insert the chamber into the magnet gap without interstitial heat shield

The magnets are mounted in a hermeticity shell serving as bearer and liquid helium tank The shell is fixed with hangers (7) inside an evacuated housing (1)

The principal parameters of the wiggler superconducting magnets are quoted in table 2 The magnet windings are made of multiwire NbTi cable wound around an oval iron core The contribution of iron to the magnet field on the axis amounts to 8 kG providing the reason to use iron inspite of occurrence of the field map dependence on excitation current

For windings fabrication a partly stabilized cable is chosen with critical current density of 55 kA/cm^2 at maximum field of 55 kG in the windings The windings are connected in series The electric stabilization of the system is provided by a proper cable choice with small enough wires diameter (15 μm) and use of monolite insulation made of fiberglass tissue impregnated with compound which prevent winding shifts The coil terminals and their connections are made of double-section superconductor with extra stabilizing coating

For pre-selection of magnets after fabrication they are installed in groups of 4 on the stand shown in fig 6 which is a model of the magnetic track The stand is plunged in liquid helium to measure the winding critical current with the field map identical to operation conditions At present the wiggler superconducting magnets are under fabrication and testing

Finally consider the problem of electric and heat protection of the superconducting wiggler windings in case transition into the normal state. To minimize liquid helium flow rate it is desirable to have only one pair of feedthrough and to connect all magnets in series. Small cable diameter is optioned However if loss of superconductivity occurs in one of them the total energy stored can

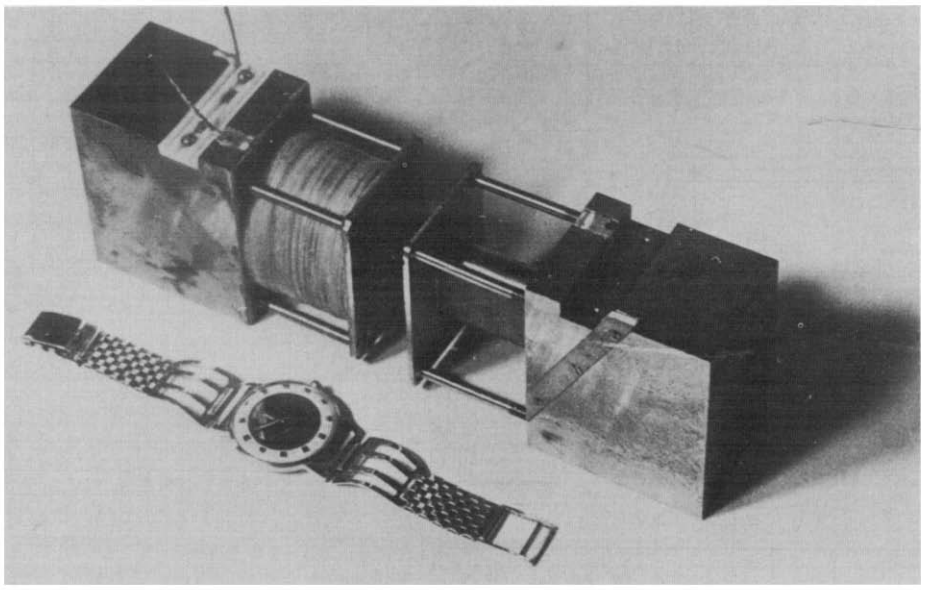

Fig 6 Stand for magnets testing

dissipate locally causing overheating of superconductor or overvoltage To avoid such a dangerous situation the wiggler is separated in sections each protected by a Si diode cooled with liquid helium (fig 7) It was discovered experimentally that the current–voltage characteristic of a usual Si diode at helium temperature displays a threshold with the threshold voltage from 5 V to 100 V and over depending on diode type, It is similar to that of a dynistor Utilization of the scheme of fig 7 enables the use of windings made of thin cable in a great number of magnets connected in series, therefore simplifying the wiggler supply and reducing the liquid helium flow rate

5. Conclusion

At present the VEPP-3 storage ring is shut down for 6 months to prepare its operation as the VEPP-4 injector

At the same time modernization of some systems is under way A new vacuum chamber is developed and manufactured for the long straight section to install the superconducting wiggler The operation of the superconducting wiggler is to begin by the end of 1978

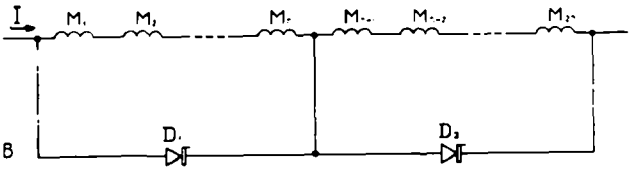

Fig 7 Electric diagram of the superconducting wingings protection using Si diodes

References

1) V L Ginzburg, Izvestiya AN SSSR seriya fizicheskaya **11** (1947) 165
2) H Motz, J Appl Phys **22** (1951) 527, **24** (1953) 826
3) G I Budker, Proc Int Conf on *Accelerators*, Yerevan (1969)
4) D F Alferov, Yu A Bashmakov and E G Bessonov, Zhurnal Tekhn Fiz **42** (1972) 1921
5) V N Bayer, V M Katkov and V M Strakhovenko, JETP **63** (1972) 2121
6) G Chu, *Parameters of the helical wiggler and synchrotron radiation*, SLAC Publication (1976) p 1782
7) G M Kulipanov and A N Skrinsky, Sov Phys Uspekhi **122** (1977) 308
8) L R Elias, W H Fairbank, J M J Madey, et al in Proc of the *Synchrotron radiation facilities*, Quebec, Summer Workshop, Quebec, 5–27 June, 1976
9) V N Bayer, V M Katkov and V S Fadin, *Izlucenive relativistikikh elektronov* (Atomizdat, Moscow, 1973)